Eur. Phys. J. B **15**, 317–326 (2000)

THE EUROPEAN
PHYSICAL JOURNAL B
EDP Sciences

One-dimensional Ising-like systems: an analytical investigation of the static and dynamic properties, applied to spin-crossover relaxation*

K. Boukheddaden[1,a], J. Linares[1], H. Spiering[2], and F. Varret[1]

[1] Laboratoire de Magnétisme et d'Optique, CNRS-Université de Versailles/St. Quentin en Yvelines, 45 avenue des États Unis, 78035 Versailles Cedex, France
[2] Institut für Anorganische Chemie und Analytische Chemie der Johannes Gutenberg-Universität Mainz, 55090 Mainz, Germany

Received 29 October 1999 and Received in final form 30 December 1999

Abstract. We investigate the dynamical properties of the 1-D Ising-like Hamiltonian taking into account short and long range interactions, in order to predict the static and dynamic behavior of spin crossover systems. The stochastic treatment is carried out within the frame of the local equilibrium method [1]. The calculations yield, at thermodynamic equilibrium, the exact analytic expression previously obtained by the transfer matrix technique [2]. We mainly discuss the shape of the relaxation curves: (i) for large (positive) values of the short range interaction parameter, a saturation of the relaxation curves is observed, reminiscent of the behavior of the width of the static hysteresis loop [3]; (ii) a sigmoidal (self-accelerated) behavior is obtained for large enough interactions of any type; (iii) the relaxation curves exhibit a sizeable tail (with respect to the mean-field curves) which is clearly associated with the transient onset of first-neighbor correlations in the system, due to the effect of short-range interactions. The case of negative short-range interaction is briefly discussed in terms of two-step properties.

PACS. 64.60.-i General studies of phase transitions – 05.70.Ln Nonequilibrium and irreversible thermodynamics – 05.50.+q Lattice theory and statistics (Ising, Potts, etc.)

1 Introduction

Pioneering works on the dynamics of spin-crossover solids have pointed out the role of interactions on the shape of relaxation curves, *i.e.* on the time dependence of the metastable state fraction [4,5] after photo-excitation of the system (according to the so-called LIESST effect [6–9]. Both phenomenologic mean-field model [4] and dynamic Monte Carlo simulations [10] have been reported to describe the experimental data. The typical feature of a self-accelerated relaxation giving the relaxation curves a sigmoidal shape [4,5,11] was assigned to the effect of interactions. In addition, a "tail" was observed and attributed to the transient onset of correlations. This tail, of course, was not obtained in the mean-field approach.

The purely molecular aspect of the relaxation has also received much attention, and the simple idea of a thermally activated process in a large temperature interval (say, above 25 K) was developed for the examples of diluted complexes [4]. Accordingly, the dynamic choice which was made to establish the first microscopic dynamic model of spin-crossover solids [12] was Arrhenius-like, rather than the widely accepted Glauber choice [13]. This choice was crucial in order to reproduce the experimental non-linear effects, *i.e.* the sigmoidal relaxation curves observed in the range 30-60 K.

The microscopic dynamic model has been treated so far in the mean-field approach. The present report is devoted to the 1-D problem, using an analytical method adapted from Huang [1] which enables the effect of correlations to be taken into account. Following recent work [3], we combine short-range and long-range interactions. In [3] the static 1-D case was solved exactly, using the analytical transfer matrix method, and the present work can be considered as its dynamic extension. The main results of [3] are summarized as follows: (i) thermal hysteresis may occur due to the combined effect of short- and long-range interactions; (ii) the shape of the hysteresis loop changes from "S" to "Z" on increasing the ratio of the short-range interaction; (iii) on (mathematically) increasing the short-range interaction parameter, the shape of the hysteresis loop tends to a limiting Z-shaped curve, the width of which closely depends on the long-range parameter.

The microscopic models developed for cooperative spin-crossover solids are based on the Ising-like Hamiltonian, following the pioneering work of Wajnsflasz and Pick [14]. Such a two-state model can be viewed as

---

* This work is dedicated to the memory of our friend Professor Olivier Kahn.

[a] e-mail: `kbo@physique.uvsq.fr`

a simple Ising model under an applied field (a temperature-dependant field to account for the different degeneracies of the levels [15]). In the dynamic Glauber approach [13], the "spins" are assumed to interact with the thermal bath, which causes them to flip randomly in time. The mean-field version of the two-level dynamic problem [12] led exactly to the phenomenological formula given by Hauser, Spiering and Gütlich [4] for the sigmoidal relaxation. Among models including correlations, Huang [1] first applied the Bethe-Peierls method to solve the Glauber problem for 1-D Ising systems under a magnetic field, and then he extended it to a Ising model for any dimension D. Here we apply his treatment to a 1-D Ising-like system which combines short- and long-range interactions.

It should be added that analytical treatments are suited to simulate the low-temperature properties of systems possessing the macroscopic energy barriers associated with the long-range interactions; alternative Monte Carlo simulations would require considerable computer times in such a case.

2 1-D Ising-like model revisited

In the Ising like model, the two states of the spin crossover molecule are represented by a fictious spin 1, with two eigenstates ±1, with respective degeneracies g_+ and g_-. In the spin crossover systems, the values $+1$ and -1 are respectively associated with the high-spin (HS) and low-spin (LS) states.

The 1D Hamiltonian including long- and short-range interactions, writes (after [3]):

$$H = -J\sum s_i s_{i+1} - \left(\frac{1}{2}k_B T \ln\frac{g_+}{g_-} - \Delta + G\langle s\rangle\right)\sum_i s_i. \tag{2.1}$$

Where: $\langle s\rangle = m$ is the net magnetization, J and G are the short and long range interactions respectively, 2Δ is the energy difference E(HS)-E(LS) for isolated molecules. g_+/g_- is the degeneracy ratio between the HS and LS states and T the temperature. The ratio g_+/g_- may be quite large (up to a few thousands) because it involves both the spin degeneracies and the density of vibrational states (see [16] and Refs. included). The Ising-like problem is reduced to the "pure Ising" one under the effective field:

$$\Delta_{\text{eff}} = \frac{kT}{2}\ln\left(g_+/g_-\right) - \Delta + Gm \tag{2.2}$$

The partition function of the 1-D "pure Ising" system is obtained by the well-known transfer matrix technique [2], and the free energy writes:

$$F = \frac{1}{2}Gm^2 - kT\ln Z. \tag{2.3}$$

The self-consistent solution of the problem is obtained by minimising the free energy with respect to m. It writes:

$$m = \frac{\sinh b}{\sqrt{\sinh^2 b + \mathrm{e}^{-4g}}} \tag{2.4}$$

where

$$b = \beta\left(Gm + \frac{k_{\mathrm{B}}T}{2}\ln\frac{g_+}{g_-} - \Delta\right) \tag{2.5}$$

$$g = \beta J. \tag{2.6}$$

The high spin fraction of molecules (n_{H}) is related to the magnetization m by:

$$n_{\mathrm{H}} = \frac{1+m}{2}\cdot \tag{2.7}$$

The static properties of this model in the case $J > 0$ have been studied by Linares *et al.* [3]: thermal hysteresis loops can occur due to the synergetic effect of short- and long-range interactions; the width of the thermal hysteresis saturates upon increasing short range interaction parameter; for large short-range interactions the thermal hysteresis loop becomes square-shaped, in agreement with the available experimental data [17].

We analyze here the conditions required for the first-order transition (spin-transition) to occur in the 1-D systems. We follow a general method recently introduced [18] which consists in comparing the equilibrium temperature of the Ising-like system (such that $m = 0$, *i.e.* equipopulated HS and LS states), given by:

$$kT_{\mathrm{eq}} = \frac{2\Delta}{\ln\left(g_+/g_-\right)}, \tag{2.8}$$

and the ordering (Curie) temperature (T_{C}) of the associated "pure Ising" system ($g_+ = g_- = 1$, $\Delta = 0$). The first-order transition occurs through the reversal of the effective field at a temperature for which the pure Ising system is ordered, thus leading to a discontinuous variation of order parameter. Consequently, the condition for obtaining the first-order transition writes:

$$T_{\mathrm{C}} > T_{\mathrm{eq}}. \tag{2.9}$$

It is easily shown that this condition, for a given value of the equilibrium temperature, leads to a threshold value for the interaction parameter. For example, in mean-field treatment (or in the particular case of the pure long range interaction, where G is substituted for zJ), the condition writes:

$$zJ > \frac{2\Delta}{\ln g_+/g_-}, \tag{2.10}$$

where J is the nearest-neighbor interaction, and z the number of these neighbors. Such a condition is found as well in the formally equivalent regular solution model of the spin transition [19] treated in the Bragg-Williams approach.

The determination of the Curie temperature of the 1-D pure Ising system combining short- and long-range interactions can be obtained using the adaptation of equation (2.4) to the pure Ising case:

$$m = \frac{\sinh\beta Gm}{\sqrt{\sinh^2\beta Gm + \mathrm{e}^{-4\beta J}}}\cdot \tag{2.11}$$

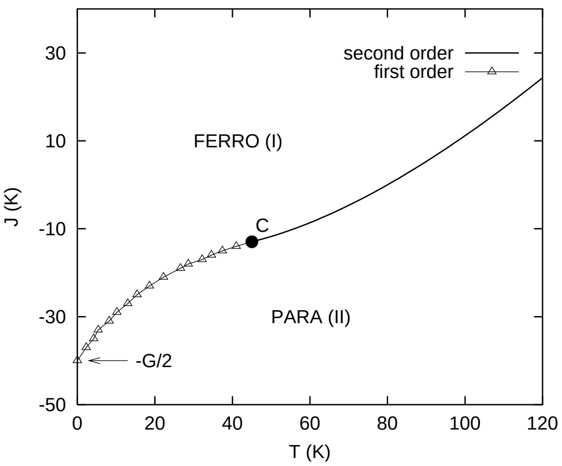

Fig. 1. Phase diagram for the 1-D Ising model ($g_+ = g_- = 1, \Delta = 0$) taking into account both long range ($G = 80$ K) and short range interactions. Full line corresponds to the the second order transition branch, and triangles concerns the first order transition. C is the tricritical point. This pure Ising phase diagram is used (see text) for determining the occurrence condition of the first-order transition of the Ising-like system: the representation point $(J, T_{\rm eq})$ should belong to the ordered phase domain. For $G = 0$ the borderline is $T_{\rm C}(J) = 0$

The Curie temperature is derived from an expansion of the previous equation around $m = 0$, giving $\beta_{\rm C} = 1/kT_{\rm C}$ through the implicit equation:

$$\beta_{\rm C} G {\rm e}^{2\beta_{\rm C} J} = 1. \tag{2.12}$$

Fortunately, the above equation explicitly provides J as a function of $T_{\rm C}$:

$$J = \frac{kT_{\rm C}}{2} \ln\left(\frac{kT_{\rm C}}{G}\right) \tag{2.13}$$

The resolution of equation (2.11) provides a second- or a first-order transition, according to the values of the interactions J and G.

For a complete discussion, we have reported in Figure 1 the computed curve $T_{\rm C}(J)$ for a given G value, where the second- and first-order branches appear, separated by a tricritical point C (this first or second order nature does not affect qualitatively the discussion which follows).

Figure 1 is interpreted as well as a phase diagram with domains for "ferromagnetic" and "paramagnetic" states separated by the borderline $T_{\rm C}(J)$ at fixed G. Then, the Ising-like system is represented by a point at coordinates $T_{\rm equil}$, J (at fixed G), and the occurrence condition for the first-order transition, according to equation (2.9), is simply that this representative point belongs to the domain of the ferromagnetic state. Therefore we now briefly describe the phase diagram of the pure 1-D Ising system.

2.1 The short-range interaction J $>$ 0

This is the case already investigated by Linarès *et al.* [3]. The phase diagram of the pure Ising system is very simple, with $T_{\rm C}$ an increasing function of J and G, as expected intuitiously. The occurrence condition for the first-order transition of the Ising-like system $T_{\rm equil} < T_{\rm C}$, can be expressed analytically as:

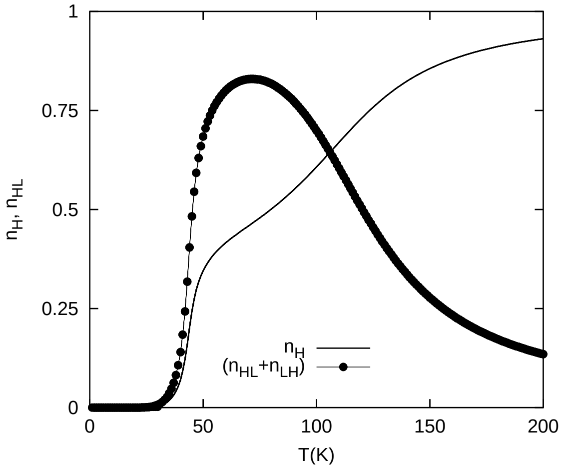

Fig. 2. High spin fraction ($n_{\rm H}$) and HS − LS fraction ($n_{\rm HL} + n_{\rm LH}$) *versus* temperature, showing a two-step conversion in the domain II of Figure 1, with $-(G+\Delta)/2 < J < -G/2$. Parameter values are $J = -60$ K, $G = 80$ K, $\Delta = 200$ K, $\frac{g_+}{g_-} = 150$.

$$J > J_{\rm C} = \frac{\Delta}{\ln g_+/g_-} \ln\left(\frac{2\Delta}{G \ln g_+/g_-}\right) \cdot \tag{2.14}$$

This equation explicits the synergetic effect of G and J, empirically observed by Linarès *et al.* [3]. For $G = 0$, $J_{\rm C}$ diverges and the 1-D Ising system does not order.

For an insufficient G value (${\rm d}T_C/{\rm d}G$ is also positive) $T_{\rm C}$ is too low, and the first-order transition does not occur. The effect of an increased short-range interaction is to raise $T_{\rm C}$, in excess of $T_{\rm equil}$, and then the first-order transition occurs above a threshold value $J_{\rm C}$.

2.2 The short-range interaction J $<$ 0.

We now consider "antiferromagnetic" short-range interactions, *i.e.* negative, which stabilize the HS − LS pairs with respect to the HS − HS, LS − LS pairs. The Ising chains with competing long range ferromagnetic and short range antiferromagnetic interactions were studied by Nagle [20]. For the spin crossover problem the "antiferromagnetic" interaction in presence of a long range "ferromagnetic" interaction was introduced to explain the experimental examples where the spin transition occurs in two steps (as termed in several studies [21–24]). Steric speculations have been proposed for this negative interaction [22].

The two-step transition (according to numerical calculations) occurs for $J < -G/2$, when the pure Ising system does not order ferromagnetically. A plateau (as shown in Fig. 3) is obtained around $m = 0$ (or $n_{\rm H} = 1/2$) because the alternate state HS − LS − HS... is stabilised and becomes a well-isolated groundstate for the pure Ising system (see Figs. 2 and 3).

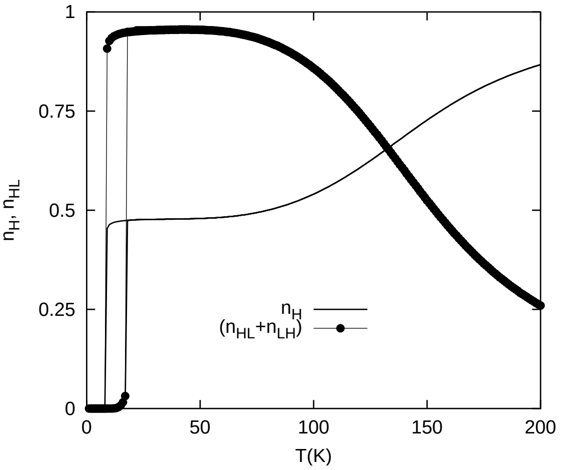

Fig. 3. High spin fraction (n_{H}) and HS − LS fraction ($n_{\mathrm{HL}}+n_{\mathrm{LH}}$) *versus* temperature, showing a two-step curve with a first-order transition and a conversion. Parameter values are $J=-100$ K, $G=80$ K, $\Delta=200$ K, $\frac{g_+}{g_-}=150$.

For $J<-(G+\Delta)/2$ the plateau starts from $T=0$, and the spin transition is termed a "half-transition". The above condition was derived from the expression of the low-temperature limit of equation (2.4), written here:

$$\lim_{\beta\to+\infty} m=\frac{-1}{\sqrt{1+\mathrm{e}^{\beta(4|J|+2Gm-2\Delta)}}}\cdot \tag{2.15}$$

The requirements for a complete two-step transition are now analysed. The low-temperature ground state LS ($m=-1$) is needed. It requires $-(\Delta+G)/2<J$. The conditions are then summarised as:

$$-(\Delta+G)/2<J<-G/2. \tag{2.16}$$

The complete phase diagram describing the two-step transition is presumably complex, as has been shown in mean-field investigation of the two-sublattice problem [15]

3 Dynamic effects

In the stochastic Glauber approach [13] the spin-flips from $s_i\to -s_i$ are induced by the thermal bath, with transition rates $W(s_i)$.

Following [13] we consider $P(\{s\};t)$ the probability of observing the system in the configuration $(s_1,...,s_N)=\{s\}$ at time t. The time evolution of $P(\{s\};t)$ is given by the master equation:

$$\begin{aligned}\frac{\partial P(\{s\},t)}{\partial t}&=-\sum_{j=1}^{N}W_j(s_j)P(\{s\}_j\,,s_j;t)\\&\quad+\sum_{j=1}^{N}W_j(-s_j)P(\{s\}_j\,,-s_j;t)\end{aligned} \tag{3.1}$$

where: $\frac{\partial P(\{s\},t)}{\partial t}$ is the flux of the probability and $\{s\}_j$ denotes the configuration of all spins excepted spin s_j.

The expectation value of the j-th spin is defined as:

$$\langle s_j\rangle=\sum_{\{s\}}s_jP(\{s\};t), \tag{3.2}$$

where the sum is taken over all spin configurations.

The detailed balance condition at equilibrium writes:

$$\begin{aligned}\frac{W(s_i)}{W(-s_i)}&=\frac{P_{\mathrm{e}}(s_1,...,-s_i,...,s_N)}{P_{\mathrm{e}}(s_1,...,s_i,...,s_N)}\\&=\frac{\mathrm{e}^{-gs_i(s_{i-1}+s_{i+1})-bs_i}}{\mathrm{e}^{gs_i(s_{i-1}+s_{i+1})+bs_i}}\end{aligned} \tag{3.3}$$

where $P_{\mathrm{e}}(s_1,s_2,...s_N)\sim \mathrm{e}^{-\beta E(s_1,...,s_i,...,s_N)}$ is the equilibrium probability and $E(s_1,...,s_i,...,s_N)$ the energy of the spin configuration $(s_1,s_2,...s_N)$.

3.1 The dynamic choice

Several dynamic choices are possible according to equation (3.3) which only provides the ratio of the probabilities of opposite transition rates. All possible choices lead to the same stable and metastable states of the system. Recently K. Boukheddaden *et al.* [12] have established that the choice suited to the spin-crossover systems was of the Arrhenius-type [25], rather than of the Glauber type [13]. The main physical reason is due to the fact that in spin-crossover systems, the dynamical process is essentially thermally activated.

Following [12], we use the identity $\mathrm{e}^{\pm\alpha}=\cosh\alpha\pm\sinh\alpha$ and the property that $s_i(s_{i-1}+s_{i+1})/2$ only takes the values ±1 or 0. Then, the Arrhenius-type transition rates are written:

$$\begin{aligned}W_{\mathrm{A}}(s_i)&\sim \mathrm{e}^{-gs_i(s_{i-1}+s_{i+1})-bs_i}\\&=\cosh b\cosh\left(gs_i(s_{i-1}+s_{i+1})\right)\\&\quad\times(1-s_i\tanh b)\left(1-\frac{1}{2}s_i(s_{i-1}+s_{i+1})\tanh 2g\right)\end{aligned} \tag{3.4}$$

The spin-flip transition rate is finally transformed as:

$$W_{\mathrm{A}}(s_i)=\frac{1}{2\tau}(x-s_ix')\prod_{\alpha=\pm1}(y-s_is_{i+\alpha}y'), \tag{3.5}$$

with the following notations: $x=\cosh b$, $y=\cosh g$, $x'=\sinh b$, $y'=\sinh g$.

We have introduced a time scale factor, $1/\tau$, resulting from a thermally activated spin flip rate, of intramolecular origin:

$$\frac{1}{\tau}=\frac{1}{\tau_0}\mathrm{e}^{-\beta E_{\mathrm{a}}^0}, \tag{3.6}$$

where $1/\tau_0$ is the individual spin flip rate between the HS to LS states, and E_{a}^0 is the intramolecular vibronic energy barrier at energy gap $\Delta=0$.

The dynamical problem of the 1-D Ising-like system is then formulated by introducing the expression (3.5) of the $W_{\mathrm{A}}(s_i)$ into the master equation (3.1). The calculation of average magnetization $m(t)$ leads to a set of 2^N coupled differential equations which involve all the correlations of the system. Of course, the exact treatment is not tractable. Then approximation methods such as mean-field [26], perturbation [27], or the local equilibrium [1] have been developed. We follow the latter, which is not restricted to the case of small external field (here the temperature-dependent field may be quite large).

3.2 The local equilibrium method (after [1])

This method is justified by the fact that the evolution time for spin-correlation functions is much larger than the individual spin-flip time. Let us consider a site s_0 with q nearest neighbors; we denote $P(s_0, n; t)$ the probability for site s_0 to be surrounded by n spins in the $+1$ state. $P(s_0, n; t)$ is assumed to be in a local statistical equilibrium even if the total system is not at equilibrium.

The method follows by taking $P(s_0, n; t)$ given by the Bethe-Peierls (BP) Hamiltonian. The cluster made of the central site s_0 and its q neighbors is considered, and the BP Hamiltonian contains the exact contribution of the isolated cluster, completed by an uniform field λ acting on the q neighbors, representing the interaction with the lattice. The BP Hamiltonian writes (with notations defined in Eqs. (2.5,2.6)):

$$\beta H^{\mathrm{Bethe}} = -g s_i \sum_{j=1}^{q} s_j - b s_i - b \sum_{j=1}^{q} s_j - \beta\lambda \sum_{j=1}^{q} s_j. \quad (3.7)$$

The occupation probabilities of the different states of the cluster are:

$$P\left(s_i, n\right) = C \binom{q}{n} \mathrm{e}^{-\beta H^{\mathrm{Bethe}}(s_i,n)}, \quad (3.8)$$

where $\binom{q}{n} = q!/n!\,(q-n)!$ is the configuration degeneracy of a cluster having n out of the q neighbors in the $+1$ state. C is a normalisation constant, which at equilibrium is the inverse of the canonical partition function. For such a cluster, the probabilities of the possible two states of the central spin are:

$$P\left(\pm 1, n\right) = C \binom{q}{n} \mathrm{e}^{\pm b} \mathrm{e}^{-q\lambda} \left(\mathrm{e}^{2\beta\lambda}\right)^n \mathrm{e}^{(b \pm g)(2n-q)}. \quad (3.9)$$

The above probabilities are time dependant. For convenience, we also make the following change of variables:

$$C_{\pm} = C \mathrm{e}^{\pm b} \mathrm{e}^{-q\lambda} \text{ and } z = \mathrm{e}^{2\beta\lambda}. \quad (3.10)$$

For the 1-D system ($q = 2$), the probabilities of the cluster states become:

$$P(\pm 1, n; t) = \frac{2}{n\,(2-n)} C_{\pm}(t) z^n(t) \mathrm{e}^{2(b \pm g)(n-1)}. \quad (3.11)$$

The Bethe-Peierls model involves further equations:

$$\sum_{n=0}^{2} \sum_{s_0=\pm 1} P\left(s_0, n; t\right) = 1, \quad (3.12)$$

which normalizes the probabilities;

$$m(t) = \sum_{n=0}^{2} \left(P(+1, n; t) - P(-1, n; t)\right), \quad (3.13)$$

which defines the local magnetization;

$$\sum_{n=0}^{2} P(+1, n; t) = \frac{1}{2} \left[\sum_{n=0}^{2} n \sum_{s_0=\pm 1} P(s_0, n; t)\right], \quad (3.14)$$

which expresses that the probability of obtaining the spin value $+1$ is the same at the central site s_0 and at the neighbor sites. This condition restores the homogeneity of the system, *i.e.* makes the local and global magnetizations identical [28].

From equations (3.11, 3.13) the following relations are obtained:

$$\begin{aligned} 1 = {} & C_{+}(t) \left(z\mathrm{e}^{(b+g)} + \mathrm{e}^{-(b+g)}\right)^2 \\ & + C_{-}(t) \left(z\mathrm{e}^{(b-g)} + \mathrm{e}^{(g-b)}\right)^2 \end{aligned} \quad (3.15)$$

$$\begin{aligned} m(t) = {} & C_{+}(t) \left(z\mathrm{e}^{(b+g)} + \mathrm{e}^{-(b+g)}\right)^2 \\ & - C_{-}(t) \left(z\mathrm{e}^{(b-g)} + \mathrm{e}^{(g-b)}\right)^2 \end{aligned} \quad (3.16)$$

and from equation (3.14):

$$z(t) \mathrm{e}^{2b} \frac{C_{-}(t)}{C_{+}(t)} = \left(\frac{z\mathrm{e}^{(b+g)} + \mathrm{e}^{-(b+g)}}{z\mathrm{e}^{b-g} + \mathrm{e}^{g-b}}\right). \quad (3.17)$$

Resolving the set of equations (3.15, 3.16), the normalization factors can be written as a function of $m(t)$ and $z(t)$:

$$C_{\pm}(t) = \frac{1 \pm m(t)}{2\left(z\mathrm{e}^{b \pm g} + \mathrm{e}^{-(b \pm g)}\right)^2} \cdot \quad (3.18)$$

Equations (3.17) and (3.18) allow a second-order equation for $z(t)$ to be obtained. The positive root of this equation is:

$$z(t) = \frac{\mathrm{e}^{-2(b+g)}}{1-m} \left[m + \sqrt{\mathrm{e}^{4g}\left(1-m^2\right) + m^2}\right]. \quad (3.19)$$

By this way $C_{\pm}(t)$ and $z(t)$ have been written as function of $m(t)$.

3.3 The two-site correlation function r(t)

The two-site correlation function $r(t)$ is defined as:

$$r(t)=\frac{1}{N}\sum_{\langle i,j\rangle}s_i s_j=\frac{N_{+\,+}-2N_{+\,-}+N_{-\,-}}{N} \tag{3.20}$$

where $N_{+\,+},N_{+\,-},N_{-\,+},N_{-\,-}$ are the number of pairs with the possible 4 configurations. The corresponding probabilities $n_{++},n_{+\,-},n_{-\,+},\ n_{-\,-}$ are defined by:

$$n_{\pm\pm}=\frac{N_{\pm\pm}}{N}\cdot \tag{3.21}$$

The normalisation relations of one-and two-spin probabilities follow:

$$n_{++}+n_{-\,-}+n_{+\,-}+n_{-\,+}=1 \tag{3.22}$$

$$n_{++}+n_{+\,-}=n_{+} \tag{3.23}$$

$$n_{-\,+}+n_{-\,-}=n_{-} \tag{3.24}$$

From equations (3.20), (3.22), (3.23), (3.24), $r(t)$ writes:

$$r(t)=4n_{++}-4n_{+}+1. \tag{3.25}$$

Taking into account that:

$$n_{+}=\sum_{n=0}^{2}P\left(+1,n;t\right), \tag{3.26}$$

and

$$n_{++}=\frac{1}{2}\sum_{n=0}^{2}nP\left(+1,n;t\right), \tag{3.27}$$

and using the expressions of $P\left(s_i,n;t\right)$, $C_{\pm}(t)$ and $z(t)$ given by the equations (3.11, 3.18, 3.19), we finally obtain:

$$r(t)=\frac{2\left(m^2-1\right)}{1+\sqrt{m^2+\left(1-m^2\right)\mathrm{e}^{4g}}}+1\cdot \tag{3.28}$$

The time dependence of the HS – LS pair probability follows:

$$n_{+-}=n_{-+}=\frac{1-r(t)}{4}\cdot \tag{3.29}$$

For the spin-crossover problem, n_{+-} (n_{-+}) is denoted n_{HL} (n_{LH}) which represents the fraction of HS – LS (LS – HS) pairs in the system.

Once $r(t)$, $C_{\pm}(t)$, $z(t)$ have been obtained, the master equation can be explicited (as follows).

3.4 The evolution equation

The time evolution of the magnetization, using equations (3.1, 3.2), writes formally:

$$\frac{\mathrm{d}\left\langle s_j\right\rangle}{\mathrm{d}t}=\frac{\mathrm{d}m}{\mathrm{d}t}=\sum_{\{s\}}s_j\frac{\mathrm{d}P\left(\{s\};t\right)}{\mathrm{d}t}=-2\left\langle s_jW(s_j)\right\rangle_t. \tag{3.30}$$

In the local equilibrium approach, the $s_jW(s_j)$ average value is obtained *via* the probabilities $P(\pm,n;t)$, by:

$$\frac{\mathrm{d}m}{\mathrm{d}t}=\sum_{n=0}^{2}\sum_{s_j=\pm1}s_jW\left(s_j\right)P\left(s_j,n;t\right). \tag{3.31}$$

Following these calculations a simple evolution equation is obtained for $m(t)$:

$$\frac{\mathrm{d}m}{\mathrm{d}t}=\frac{1}{\tau}\left(z(t)\mathrm{e}^{b}+\mathrm{e}^{-b}\right)^2\left(C_{-}(t)\mathrm{e}^{b}-C_{+}(t)\mathrm{e}^{-b}\right). \tag{3.32}$$

In the steady state, this equations exactly gives the static Bethe-Peierls equation.

Substituting in equation (3.32) the expressions of $C_{\pm}$ and z, given by equations (3.18, 3.19), the explicit form of the evolution equation follows:

$$\frac{\mathrm{d}m}{\mathrm{d}t}=-\frac{1}{\tau_0}\mathrm{e}^{-\beta E_a^0}\mathrm{e}^{-2g}\times\left\{m\cosh b-\sinh b\ \sqrt{m^2+\left(1-m^2\right)\mathrm{e}^{4g}}\right\} \tag{3.33}$$

with b, g defined in equations (2.5, 2.6).

3.5 Static limit

For $\frac{\mathrm{d}m}{\mathrm{d}t}=0$, equation (3.33) yields:

$$m=\frac{\sinh b}{\sqrt{\sinh^2 b+\mathrm{e}^{-4g}}}. \tag{3.34}$$

This exactly is the equation obtained by Linares *et al.* [3] using the well-known transfer matrix method. Such a result was expected, since the Bethe-Peierls model gives the exact solution of an infinite chain in the two state Ising model (as well as for the three-state $s=\pm1,0$ Ising model [29]).

4 Results and discussion

We analyze here the shape of the relaxation curves of the high-spin fraction at low temperatures (after photo-excitation).

At low temperatures, we have $2\sinh b\simeq-\mathrm{e}^{-b}$ and $2\cosh b\simeq\mathrm{e}^{-b}$, since $\beta(E_{\mathrm{a}}^0+b)\simeq\beta\left(E_{\mathrm{a}}^0-\varDelta+Gm\right)\ll\beta(E_{\mathrm{a}}^0-b)\simeq\beta\left(E_{\mathrm{a}}^0+\varDelta-Gm\right)$. Then equation (3.33) can be transformed as:

$$\frac{\mathrm{d}m}{\mathrm{d}t}\simeq-\frac{1}{2\tau_0}\mathrm{e}^{-\left(\beta E_{\mathrm{a}}^0+b\right)}\left(m\mathrm{e}^{-2g}+\sqrt{m^2\mathrm{e}^{-4g}+\left(1-m^2\right)}\right). \tag{4.1}$$

Because b depends on m, and due to the complex form of equation (4.1), the general case is not analytically tractable. Therefore we start with a few particular cases (J or $G=0$) for which the analytical resolution is possible.

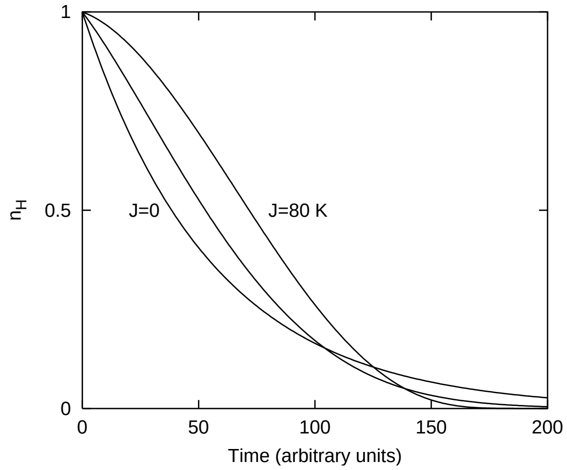

Fig. 4. Relaxation curves of the high-spin fraction for different positive values of the short range interaction J in the case $G = 0$. Parameter values are: $E_a = 1500$ K, $\Delta = 1563$ K, $\frac{g_+}{g_-} = 4675$, $T = 70$ K, $J = 0$, 30, 80 K (from left to right side). The arbitrary time unit is $1/\tau_0$. The parameter values in this case correspond to the chain compound [Fe(Htrz)$_2$(trz)] BF$_4$ [3,18]. It is interesting to note the tail effect on the relaxation as well the sigmoidal shape which increases with the interaction parameter J.

4.1 The long-range interaction case (J = 0)

In this case $g = 0$ and there only remains the long range interaction, *i.e.* the mean field case. Only $G > 0$ has to be considered, according to the elastic theory of long-range interaction in spin-crossover solids [30]. The previously established [12] equation is derived:

$$\frac{\mathrm{d}m}{\mathrm{d}t} = -\frac{1}{2\tau_0}\mathrm{e}^{-\beta E_a^0}(m\ \cosh b(m) - \sinh b(m)). \quad (4.2)$$

As already shown [12] in this low-temperature case, this mean-field evolution equation is equivalent to the phenomenological Hauser equation [4]:

$$\frac{\mathrm{d}n_H}{\mathrm{d}t} \simeq -Kn_H\mathrm{e}^{-\alpha n_H}. \quad (4.3)$$

The correspondence with the Hauser self-acceleration parameter is:

$$\alpha = 2\beta G. \quad (4.4)$$

4.2 The J > 0 short-range case

A "ferromagnetic" interaction, with $J > 0$, favors pairs in the same state, *i.e.* HS-HS and LS-LS pairs. It is then expected that, starting from a saturated metastable HS state, the relaxation to the stable LS state will be slowed down at the beginning ($m > 0$). On the contrary, the end of the relaxation will be accelerated by the effect of the cooperative interaction. This is a basic mechanism for the self-accelerated relaxation, acting in the same sense as the mean-field effect of long-range interaction (previous section).

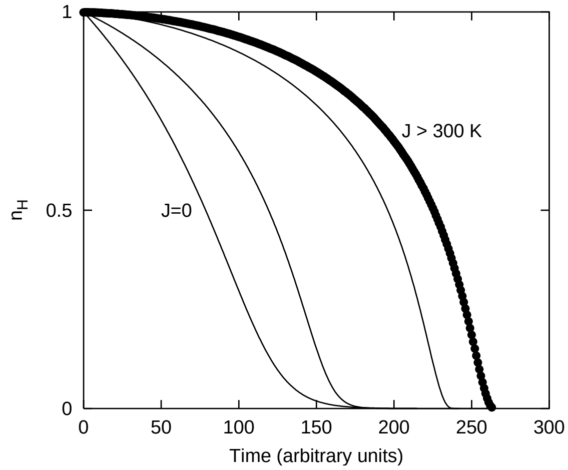

Fig. 5. The effect of a large J on the relaxation curves. From left to right, J values are: 0, 30, 100, 300, 500 K. $G = 100$ K and the other parameters are those of Figure 4. Note the saturation effect in this relaxation curves for high values of J. For example the $J = 300$ K and 500 K curves are almost superimposed.

4.2.1 The "ferromagnetic" pure-short-range case (G = 0, J > 0)

Figure 4 shows the relaxation behavior for this case. The sigmoidal shape can be obtained, *i.e.* it does not require the effect of long-range interaction, as expected from the above qualitative approach. The sigmoidal shape, characterized by an inflexion point, requires:

$$J > \frac{kT}{4}\ln 2 = J_c. \quad (4.5)$$

We now investigate the behavior of the relaxation curves for large increasing values of J. Equation (3.34) shows the saturation of $\mathrm{d}m/\mathrm{d}t$ as function of $g = J/k_BT$. The limiting equation (for $J \to \infty$) is:

$$\frac{\mathrm{d}m^\infty}{\mathrm{d}t} = -\frac{1}{2\tau_0}\mathrm{e}^{-\left(\beta E_a^0 + b\right)}\sqrt{1-m^2}, \quad (4.6)$$

and leads to a "saturation" behavior (also valid for $G \neq 0$, see Fig. 5) which compares to the static saturation previously reported [3] for the width of the thermal hysteresis loop.

4.2.2 The "ferromagnetic" general case (G > 0, J > 0)

For $G > 0$ the relaxation curves are systematically sigmoidal for $G > kT/2$, see Figure 5. Also, $\mathrm{d}m/\mathrm{d}t$ becomes

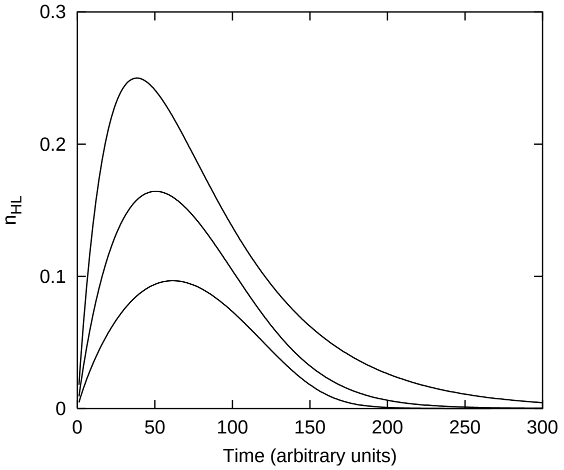

Fig. 6. Time evolution of the HS – LS pair fraction ($n_{\mathrm{HL}}(t)$) corresponding to the case shown in Figure 4. $G = 0$, $J = 0, 25, 50$ K from top to bottom. The short range interaction stabilizes the LS – LS – LS... phase at low temperature, and therefore reduces the value of the maximum of $n_{\mathrm{HL}}(t)$. The arbitrary time unit is $1/\tau_0$.

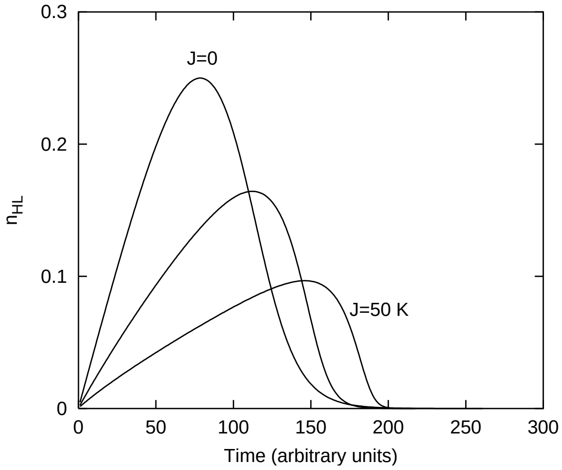

Fig. 7. Effect of the short-range interaction on the time-dependence of $n_{\mathrm{HL}}(t)$; $G = 100$ K, same case as Figure 5. From top to bottom the J values are: 0, 25, 50 K. The arbitrary time unit is $1/\tau_0$. Comparison to Figure 6 shows that the effect of J is enhanced by the presence of $G \neq 0$.

independent of J for $\beta J = g \gg 1$. In this case the dynamic properties only depend on the long-range interaction parameter G, as shown by the limiting evolution equation:

$$\frac{\mathrm{d}m^{\infty}}{\mathrm{d}t} = -\frac{1}{2\tau_0}\mathrm{e}^{-\beta\left(E_{\mathrm{a}}^0+\frac{kT}{2}\ln\left(\frac{g_+}{g_-}\right)-\Delta\right)}\sqrt{1-m^2}\,\mathrm{e}^{-\beta G m}. \tag{4.7}$$

This equation slightly differs from the mean-field expression [4,12]:

$$\left(\frac{\mathrm{d}m}{\mathrm{d}t}\right)_{\mathrm{MF}} \cong -K\left(1+m\right)\mathrm{e}^{-\beta G m} \tag{4.8}$$

where K is a constant dependant on the coupling parameters, the crystal field splitting and the degeneracy ratio.

The dynamic behavior can be discussed with respect to the time dependence of the pair occupation probabilities, see Figure 6 where the ratio of HS – LS pairs ($n_{+-}+n_{-+}$) is shown for different values of the short-range interaction parameter J. The curves exhibit maxima which approximatively correspond to the transient situation $m(t) = 0$. An increased interaction J lowers the maximum of the correlation curve because it more strongly stabilises the HS – HS and LS – LS pairs with respect to the HS – LS pairs. Also, it slows down the onset of these HS – LS correlations which are involved in the relaxation of $m(t)$. The relationship between the hindrance of these correlations and the initial slowing down of the relaxation of $m(t)$ (compare Figs. 4 and 6) illustrates the coupling effect between $r(t)$ and $m(t)$ which governs the evolution of the system.

Also, the effect of the long-range interaction on the correlations can be discussed, see Figures 5 and 7. The effect of the long-range interaction is to increase the life-time of the metastable state HS – HS – HS..., and to "stabilise" the pair probabilities, tending to give them the random values consistent with the transient $m(t)$ value.

4.3 The J < 0 short-range case

An "antiferromagnetic" short-range interaction, with ($J < 0$), favors the HS – LS with respect to symmetric pairs. It competes against the long range "ferromagnetic" interaction, thus leading (as shown above) to static two-step transitions. Accordingly, we expect transient behaviors of $n_{\mathrm{HS}}(t)$, occurring in two steps, as suggested by previous Monte Carlo simulations [10] on 3-D systems.

4.3.1 The pure short-range case ($\mathbf{G = 0, J < 0}$)

In the absence of long-range interactions, b becomes independent of m, and we conveniently re-write equation (4.1) in the following form:

$$\frac{\mathrm{d}m}{\mathrm{d}t} \simeq -\frac{1}{2\tau_0}\mathrm{e}^{-\left(\beta E_{\mathrm{a}}^0+b\right)}\left(m\mathrm{e}^{2|g|}+\sqrt{m^2\mathrm{e}^{4|g|}+\left(1-m^2\right)}\right). \tag{4.9}$$

This equation shows that for $m \cong 1$, the short-range "antiferromagnetic" coupling tends to speed up the decay of the HS fraction, the rate of which is limited by the maximum value $1/\tau_0$. The equation also shows that $m = \pm 1$ are stationary values for $m(t)$. However, at variance from the cooperative case, there is no saturation effect for large $|J|$ values. Indeed, in this case $|g| \gg 1$ values,

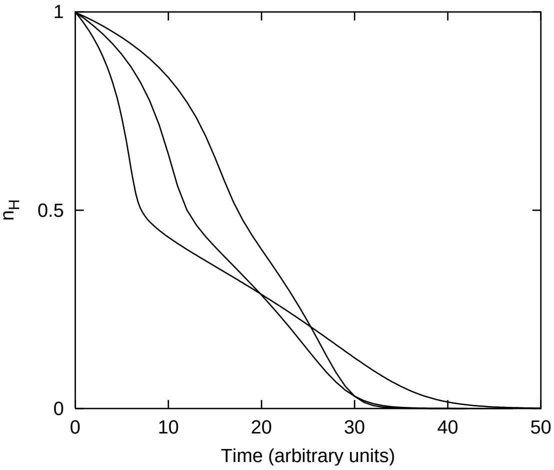

Fig. 8. Relaxation curves of high-spin fraction in a two-step transition case for different values of the "antiferromagnetic" short-range interaction. The parameter values are: $T = 25$ K, $\Delta = 1563$ K, $g_+/g_- = 4675$, $E_a = 1500$ K, and from left to right: $J = -35$, -28, -23 K respectively. The arbitrary time unit is $1/\tau_0$.

equation (4.9) transforms:

$$\frac{\mathrm{d}m}{\mathrm{d}t} \simeq -\frac{1}{2\tau_0}\mathrm{e}^{-\left(\beta E_\mathrm{a}^0 + b\right)} m \mathrm{e}^{2|g|}. \tag{4.10}$$

Then, the asymptotic state at large times t is the state $m = 0$ corresponding to $n_\mathrm{HL} + n_\mathrm{LH} = 1$; the ground state of a pair is the HS − LS state, irrespective of the state of the surroundings.

An analytical investigation shows the absence of inflexion points on the $m(t)$ curve, which consequently does not exhibit (for $G = 0$) the sigmoidal character for any $J < 0$.

4.3.2 The general case ($G > 0, J < 0$)

The long-range and short-range interactions compete against each other, both at short and long times. At short times, starting from $m \cong 1$, the long-range interaction tends to slow down the relaxation, while the short-range interaction tends to speed it up. At long times, the long-range interaction tends to speed up the relaxation towards the LS state, while the short-range interaction tended to stabilize the intermediate HS − LS state of the pairs. Then, moderate $|J|$ values will slow down the relaxation to the LS − LS state, *i.e.* the relaxation of $m(t)$ towards zero. On increasing $|J|$ value, the approach to the stabilisation of the $m = 0$ ($n_\mathrm{H} = 0.5$) state will induce a two-step shape in the $m(t)$ curve, as shown in Figure 8, in agreement with the Monte Carlo simulations reported in [10].

5 Perspectives and conclusion

The relaxation behavior of the system depends on the initial values of both the HS fraction, $m(t = 0)$ and the first-neighbor correlation $r(t = 0)$. In more general terms, it depends on the past thermo-optical history of the system. First-neighbor correlations, at least, are for this an important parameter. Convincing experiments on the effect of the building up of correlations, previous to the relaxation process, have been reported in [10], together with their successful modelling by Monte Carlo simulations. Obviously a similar work is possible using the present analytical formulation. Since even more information should be obtained from dilute systems, an extension of the model is in progress.

In the present work, the Huang local equilibrium approach has been applied to the 1-D lattice. The question of dimensionality in spin-crossover systems in not straightforward, since the mechanism for the short-range interaction is not yet solved. Qualitatively, the short-range interaction is usually considered as "steric" in nature, *i.e.* electrostatic far beyond the dipole approximation, but it might also come from the chemical bonding in the case of polymeric materials which also exist in 1-D and 2-D lattices. Quite recently, 1-D polymeric systems have been prepared, pure and diluted in a spin-crossover inactive homologous [31]. Their dynamic properties are under study and will be analysed in the frame of the present model, with a special interest in the behavior of the correlations.

We acknowledge Professor T. Luty for useful discussions, Dr. J. Hodges for a critical reading of the manuscript. LMOV is supported by CNRS, as "Unité Mixte de Recherche" (UMR *n*° 8634). The CEE financial support (TMR action TOSS, contract *n*° ERB-FMRX-CT98-0199) is acknowledged.

References

1. H.W. Huang, Phys. Lett. A **48**, 395 (1974), see also: H.W. Huang, Phys. Rev. A **8**, 2553 (1973).
2. J.M. Yeomans, in *Statistical Mechanics of Phase Transitions* (Oxford University Press, 1992).
3. J. Linares, H. Spiering, F. Varret, Eur. Phys. J. B **10**, 271 (1999).
4. A. Hauser, P. Gütlich, H. Spiering, Inorg. Chem. **25**, 4345 (1986).
5. A. Hauser, J. Chem. Phys. **94**, 2741 (1991).
6. S. Decurtins, P. Gütlich, C.P. Köhler, H. Spiering, A. Hauser, Chem. Phys. Lett. **1**, 139 (1984).
7. P. Gütlich, A. Hauser, H. Spiering, Angew. Chem. Int. Ed. Engl. **33**, 2024 (1994).
8. A. Hauser, Comments Inorg. Chem. **17**, 17 (1995).

9. A. Hauser, Coord. Chem. Rev. **11**, 275 (1991).
10. H. Romstedt, H. Spiering, P. Gütlich, J. Phys. Chem. Solids **59**, 1353 (1998).
11. A. Desaix, O. Roubeau, J. Jeftic, J.G. Hassnoot, K. Boukheddaden, E. Codjovi, J. Linarès, M. Noguès, F. Varret, Eur. Phys. J. B **6**, 183 (1998).
12. K. Boukheddaden, I. Shteto, B. Hôo, F. Varret, Phys. Rev. B (in revision).
13. R.J. Glauber, J. Math. Phys. **4**, 294, (1963).
14. J. Wajnflasz, R. Pick, J. Phys. Colloq. France **32**, C1-537 (1971).
15. S. Doniach, J. Chem. Phys. **68**, 11 (1978), M. Nielsen, L. Miao, J.H. Ipsen, O.G. Mouritsen, M.J. Zuckermann, Phys. Rev. E. **54**, 6889 (1996).
16. A. Bousseksou, H. Constant-Machado, F. Varret, J. Phys. I France **5**, 747 (1995).
17. J. Kröber, J.P. Audière, R. Claude, E. Codjovi, O. Kahn, J.G. Haasnoot, F. Grolière, F. Jay, A. Bousseksou, J. Linares, F. Varret, A. Gonthier-Vassal, Chem. Mater. **6**, 1404 (1995).
18. I. Shteto, K. Boukheddaden, F. Varret, Phys. Rev. E **60**, 5139 (1999).
19. C.P. Slichter, H.G. Drickamer, J. Chem. Phys. **56**, 2142 (1972).
20. J. F. Nagle, Phys. Rev. A **2**, 2124 (1970).
21. R. Jakobi, H. Spiering, P. Gütlich, J. Phys. Chem. Solids **53**, 267 (1992).
22. C.P. Köhler, R. Jakobi, E. Meissner, L. Wiehl, H. Spiering, P. Gütlich, J. Phys. Chem. Solids **51**, 239 (1990).
23. J.A. Real, H. Bolvin, A. Bousseksou, A. Dworkin, O. Khan, F. Varret, J. Zarembovitch, J. Amer. Chem. Soc. **114**, 4650 (1992).
24. A. Bousseksou, J. Nasser, J. Linarès, K. Boukheddaden, F. Varret, J. Phys. I France **2**, 1381 (1992).
25. M. Suzuki, R. Kubo, J. Stat. Phys. **15,** 233 (1976).
26. M. Suzuki, R. Kubo, J. Phys. Soc. Jpn **24**, 51 (1968).
27. K. Kawasaki, T. Yamada, Prog. Theor. Phys. **39**, 1 (1968).
28. A. Bethe, Proc. Roy. Soc. A **150**, 552 (1935).
29. T. Obokata, T. Oguchi, J. Phys. Soc. Jpn **25**, 322 (1968).
30. N. Willenbacher, H. Spiering, J. Phys. C **21**, 1423 (1988), see also H. Spiering, N. Willembacher, J. Phys. Cond. Matter **1**, 10089 (1989).
31. Results presented in *the 4th Spin Crossover European Family Meeting in Seeheim* (Germany, 1999).